Supplementary Information

Conformation-dependent charge transport through short peptides

*Davide Stefani,[†, §] Cunlan Guo,[‡, §, ¶, *] Luca Ornago,[†] Damien Cabosart,[†] Maria El Abbassi,[†] Mordechai Sheves, David Cahen,[‡] and Herre S. J. van der Zant[†, *]*

[†]Kavli Institute of Nanoscience, Delft University of Technology, Delft, The Netherlands

[‡]Materials and Interfaces, Weizmann institute of Science, Rehovot, Israel

[¶]Current address: College of Chemistry and Molecular Sciences, Wuhan University, No. 299 Bayi road, Wuhan, Hubei, P.R China, 430072

[§]These two authors contributed equally to this work

Email: cunlanguo@whu.edu.cn; h.s.j.vanderzant@tudelft.nl

Keywords: Mechanically controlled break-junctions, single-molecule, oligopeptide, molecular electronics

Contents:

I. Characterization of the bare gold device

Before each measurement, we characterize the bare device before drop-casting the peptide solution to ensure that the electrodes are clean and well aligned. This is done by recording 2 000 consecutive breaking traces in ambient (air and room-temperature) conditions. The characterization of the bare device used for the measurements of 3Ala in the main text is shown in Fig. S1, *i.e.*, it is the same junction before drop-casting the 3Ala solution. The traces show a clear plateau at a conductance of 1 G_0, a sudden drop in conductance due to the snapback of the electrodes, and finally an exponential decay in conductance with the electrode displacement. No additional step-like features are present (see also Figs. S1b and S4).

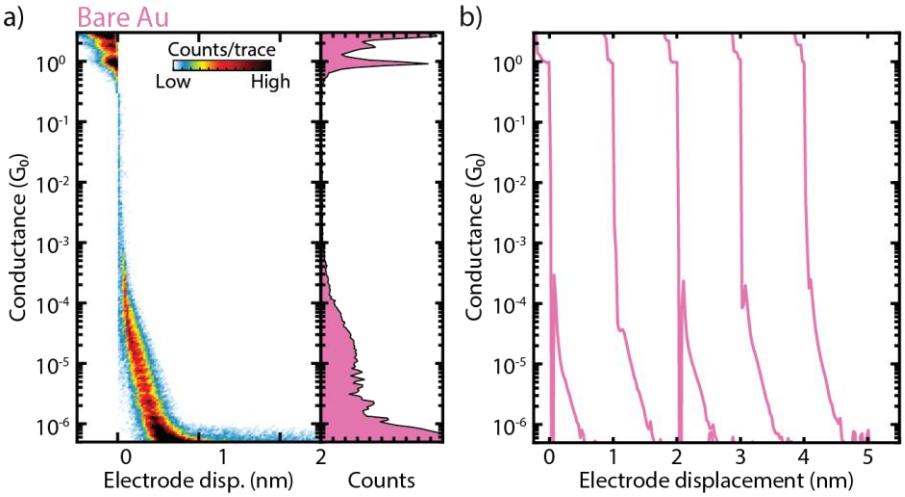

Figure S1. a) Two-dimensional (left panel) and one-dimensional (right panel) conductance histogram built from 2 000 consecutive breaking traces collected on a bare device before deposition of the molecular solution and displayed without data selection (same device as used for the measurements of 3Ala shown in Fig. 2a). The applied bias is 100 mV and the electrode speed is 6 nm/s. b) Examples of breaking traces recorded on this bare device.

II. Measurements of (*n*)Ala series

Figures. S2a and S2c shows two-dimensional histograms of the peptides 2Ala and 3Ala, whereas Fig. S2e shows the result of the measurement for 4Ala. The concentration of the molecular solutions drop-casted was 2 μM in all cases. The 2D histograms contain consecutive traces and are obtained without any data selection; these datasets are the input for the clustering algorithm.

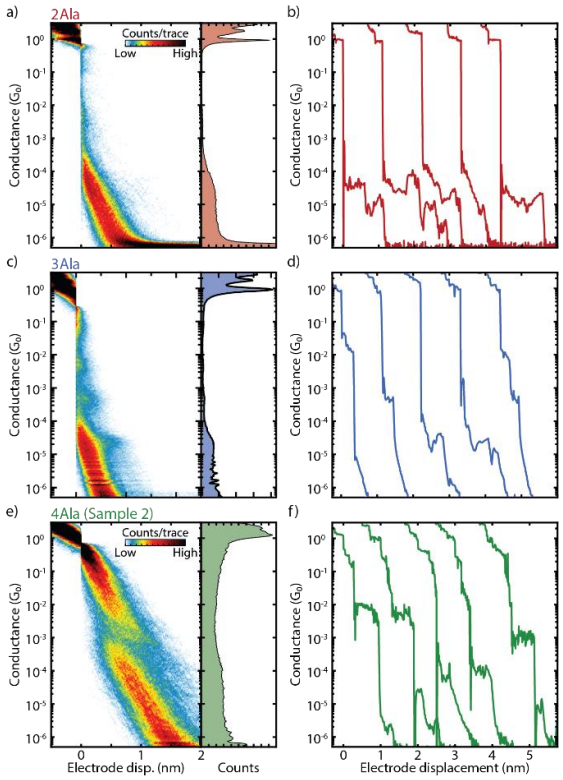

Figure S2 Two-dimensional (left panel) and one-dimensional (right panel) conductance histograms with no data selection of 2Ala (a), 3Ala (c) and 4Ala (e). (b), (d), and (f): Examples from the 2 000 consecutive breaking traces collected for each molecule. For 3Ala, 10 000 traces have been collected instead. The applied bias is 100 mV and the electrode speed is 2 nm/s for 2Ala, 3 nm/s for 3Ala, and 3 nm/s for 4Ala.

III. Measurements of 4-amino-acid series

Figures. S3a, S3c, and S3e show the unfiltered two-dimensional and corresponding one-dimensional histograms of the peptides 3Ala-Trp, 3Ala-Cys and 2Ala-Trp-Cys; Figures. S3b, S3d, and S3f show examples of individual breaking traces. The concentration of the molecular solutions drop-casted was 2 μM in all cases. The two-dimensional histograms present counts in the whole conductance range.

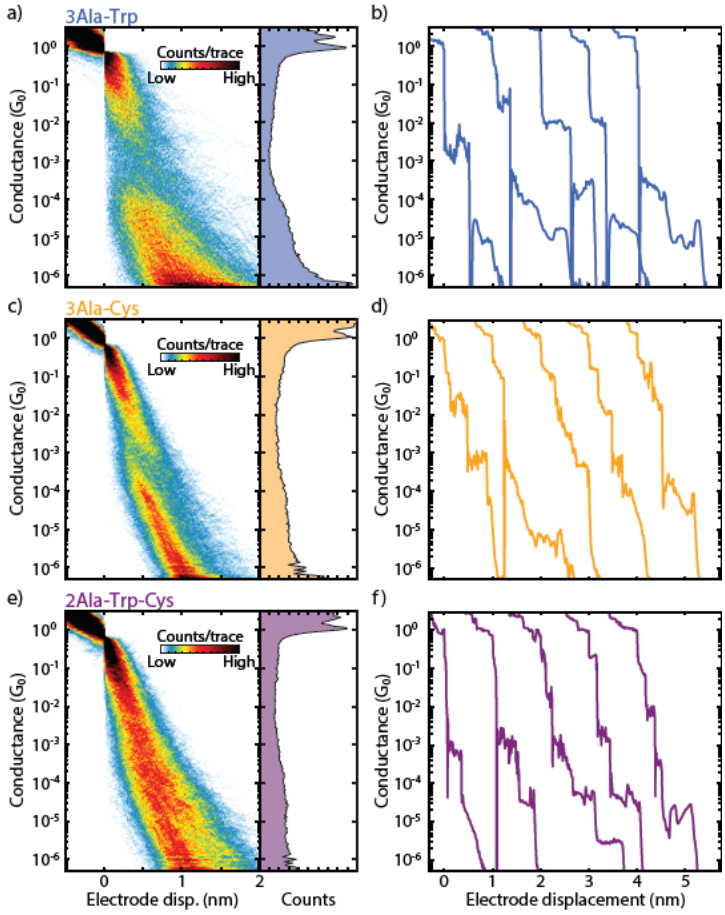

Figure S3. (a), (c), and (e): Two-dimensional (left panel) and one-dimensional (right panel) conductance histograms with no data selection of 3Ala-Trp (a), 3Ala-Cys (c), and 2Ala-Trp-Cys (e). (b), (d), and (f): Examples of the 2 000 consecutive breaking traces collected for each molecule. The applied bias is 100 mV and the electrode speed is 4 nm/s for 3Ala-Trp, 3 nm/s for 3Ala-Cys, and 2 nm/s for 2Ala-Trp-Cys.

IV. Clustering parameters

To help analyzing the 2D-histograms, we employ a reference-free classification algorithm based on clustering of the data with the K-means++ method (Figs. 2c and 2d). From each trace, a 28-by-28 two-dimensional histogram and a 100-bin one-dimensional histogram are extracted. These are then combined to form the 884-dimensional feature space over which the clustering algorithm operates. The 28-by-28 images are constructed, spanning the conductance range from 0 to -6 $\log(G/G_0)$, and displacement between 0 and 1.5 nm. For the creation of the one-dimensional histogram the conductance ranges from 1 to -7 $\log(G/G_0)$, and the trace is interpolated to have 1 000 points in the same displacement range. The addition of the 1D-histogram curve gives more weight to the plateaus in the traces and thus helps with their classification; the method is similar to the previous reported work[1]. The K-means++ algorithm is then run 100 times with randomly initialized conditions and the result that yields the smallest cost function value is used.

The datasets were split in 15 classes for the analysis presented in the paper, and the dataset of 3Ala was divided in 5, 7, 9, 11, 13, 15, 17, 20 classes, to study the influence of the number of clusters on the analysis. The 1D-histogram of classes showing plateaus in the corresponding 2D-histogram were then fitted with a log-normal distribution. To keep the analysis as consistent as possible, only the most prominent peak in each histogram was fitted. For two cases we show all 15 clusters below[2]: Figure. S5 displays the 15 classes for the 3Ala data set shown in the main text (Fig. 2a), while Fig. S4 shows the 15 classes of the same device prior to molecule deposition. Importantly, in the latter case, neither peaks in the one-dimensional histograms nor conductance plateaus in the two-dimensional ones are present.

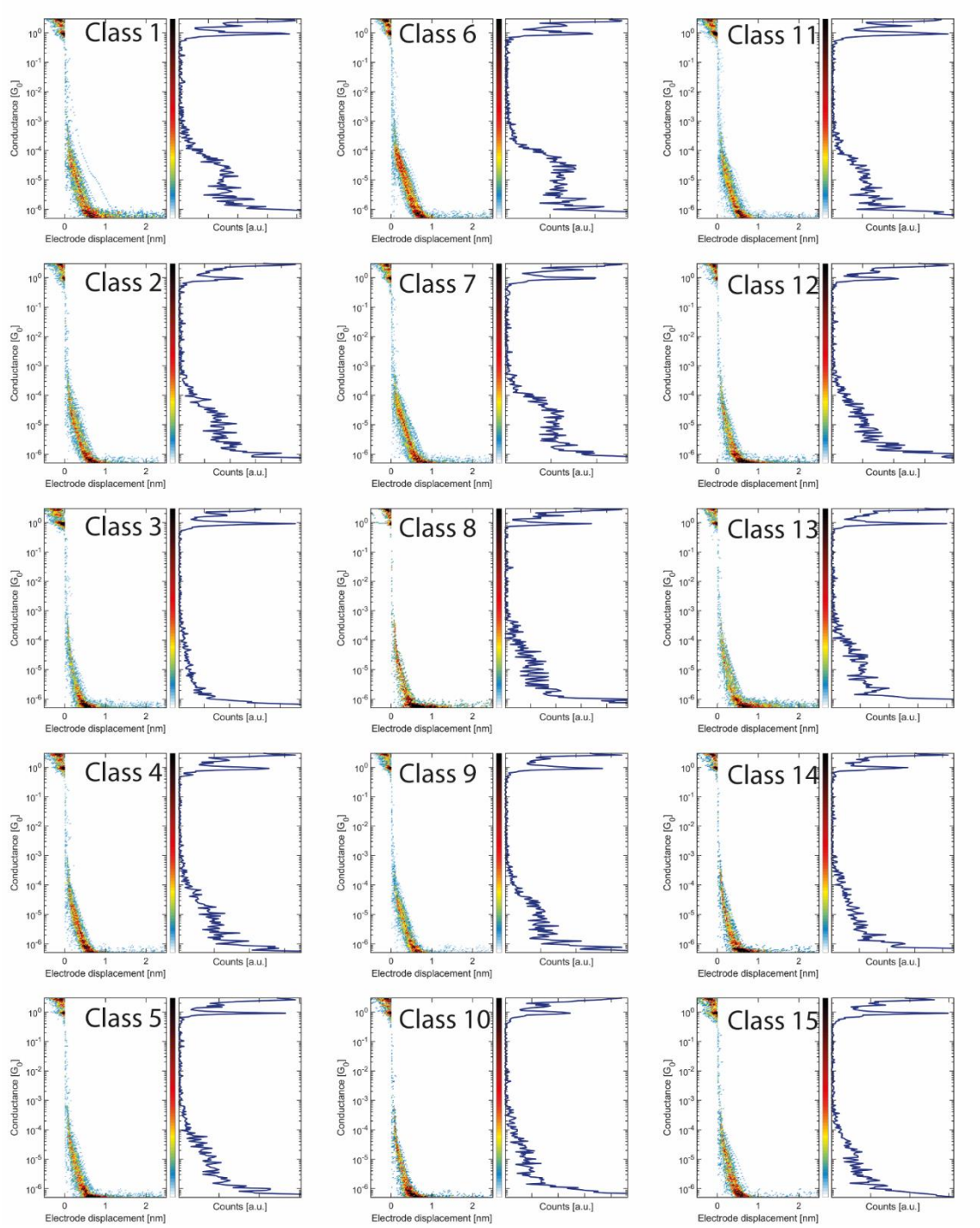

Figure S4. All classes resulting from splitting a dataset of 2 000 traces, measured on clean sample before the drop casting of 3Ala. Note that none of the clusters show step-like features, nor peaks in the 1D histogram.

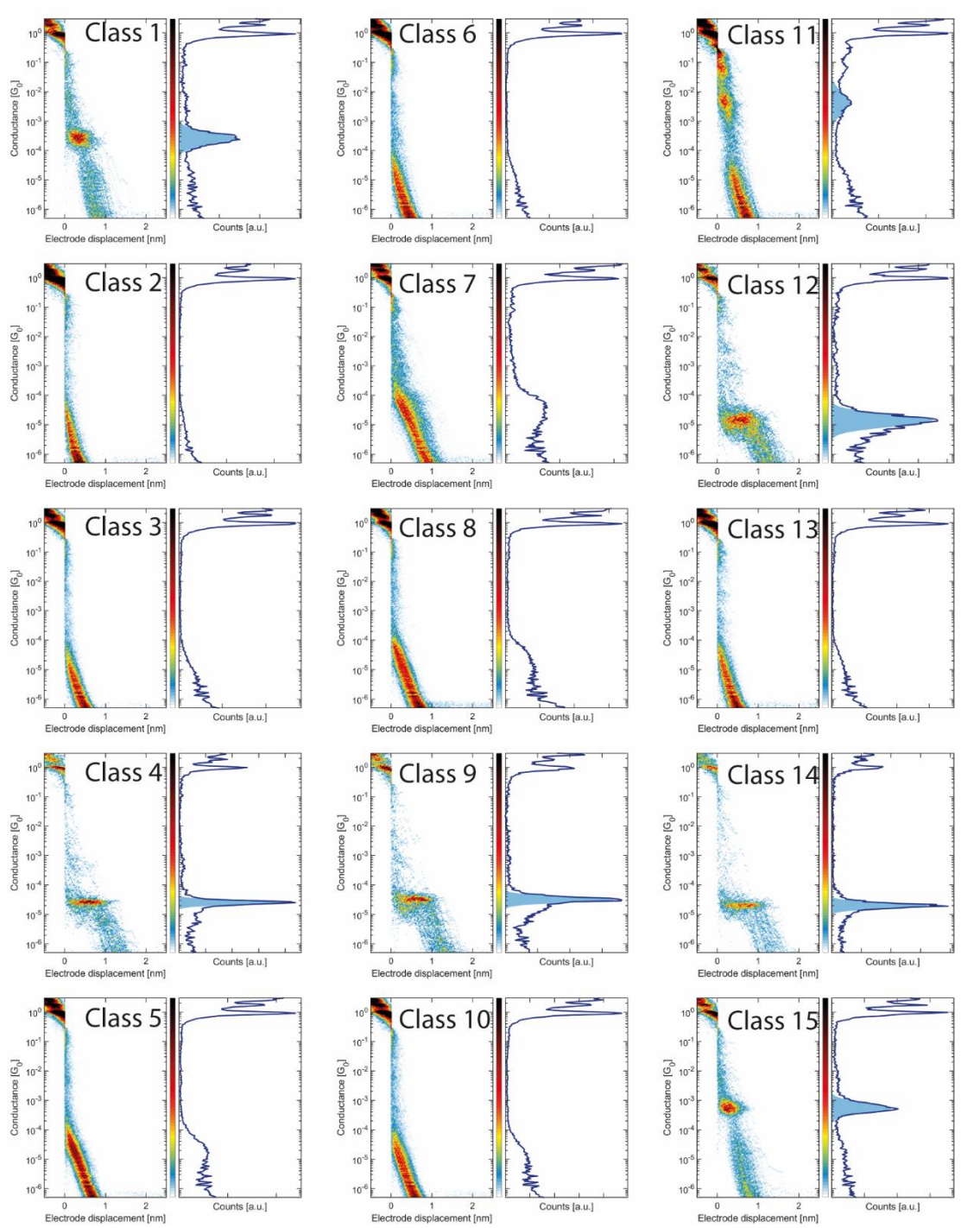

Figure S5. All classes resulting from splitting the 3Ala dataset of the main text (Fig.2) in 15 clusters. The blue shaded areas under the one-dimensional histogram represent the best fit to the data of the identified peaks.

V. Plateau length and position

As mentioned in the main text, the position and length of the plateau associated with a cluster are determined from the average portion of each individual trace that falls within 3 times the

standard deviation of the cluster peak. A schematic of this procedure is shown in Fig. 3a. The length of the plateaus could alternatively be extracted by considering another window of interest (*W*). As an example, Fig. S6 shows the results obtained by using a fixed width of 1 decade (red dots). While the absolute values of the plateau length are affected by the choice of the window of interest, mostly overestimating the size of shorter plateaus, the plateau conductance vs. plateau length distribution displays the same overall behavior (Fig. S6b). The position of the plateau, on the other hand, is hardly affected by the choice of *W* (Fig. S6a). This can be intuitively understood: the position as well as the plateau conductance is defined as the middle point of the plateau, centered around which the window of interest is defined; changing *W* symmetrically will then yield the same middle point, as long as only 1 plateau falls into the window. There is another advantage in using the plateau position instead of the plateau length. In the case of traces showing multiple plateaus (Figs. S2 and S3), the plateau length would be insensitive to whether the same plateau appears by itself in a trace, or if it is preceded by other plateaus in the trace. On the other hand, the plateau position would be higher in the latter case.

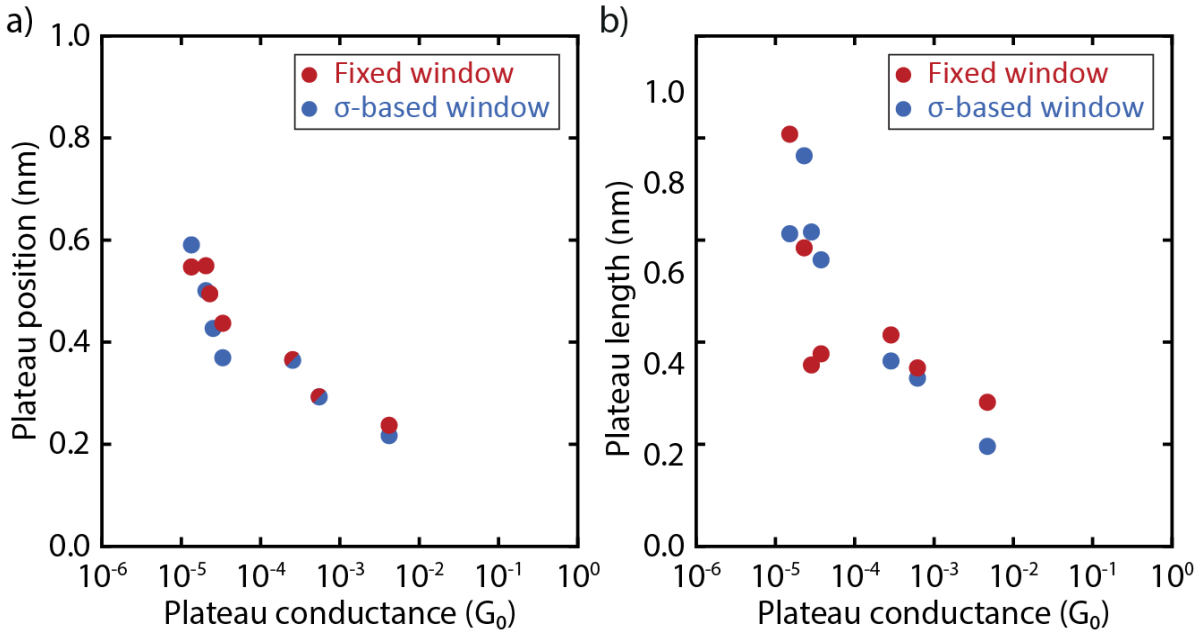

Figure S6. a) Conductance vs. plateau position and b) conductance vs. plateau length where the values on the y-axis are computed using two different methods: with a fixed width window (red) or with a "dynamic" window of 3 times the standard deviation of the fit.

VI. Estimation of the plateau conductance vs. plateau position slope, γ

The length decay (so-called β) parameter is usually determined by measuring the most probable conductance of several molecules composed of different numbers of a repeating subunit (and therefore with different length). In the case of the peptides presented in this work, however, the presence of multiple configurations and the subsequent absence of a single conductance value associated to the molecule, makes it less meaningful to estimate the traditional beta factor of amides from the measurements of 2Ala, 3Ala and 4Ala. For this reason, we only report on the slope of the plateau conductance vs. plateau position, which we denote as γ, which can be seen as

an effective length dependent factor to compare the conductance of the peptides[3, 4] and alkanes [5-8] with different length to other measurements.

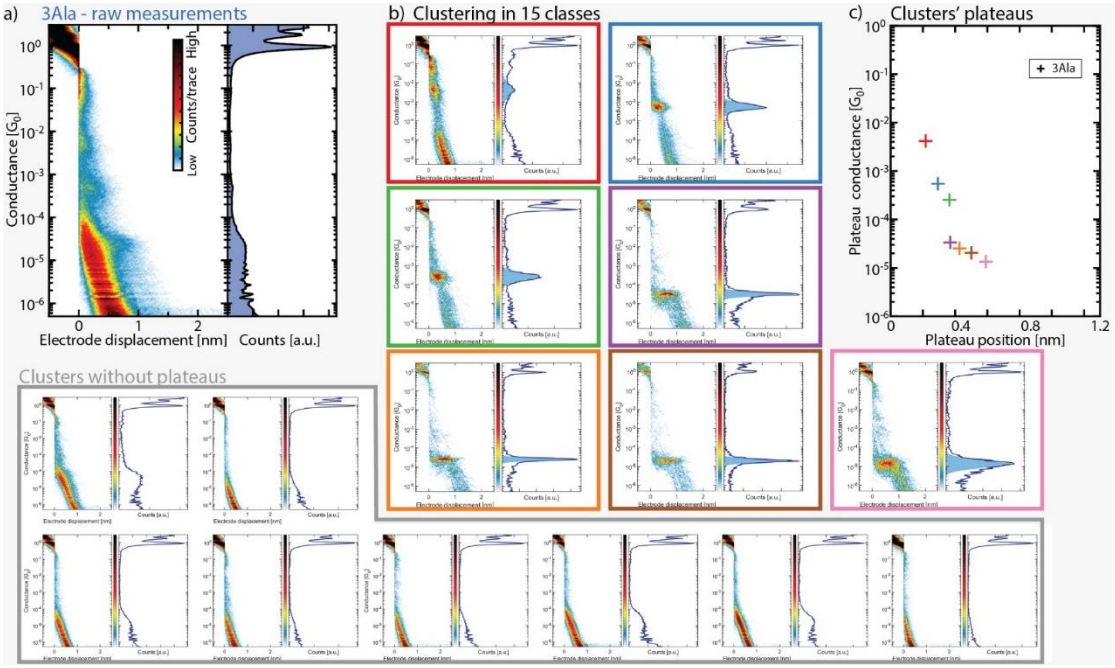

Figure S7. General workflow of the analysis performed: a) Raw data of the measurements performed on 3-Ala as an example. Every single trace of the histogram is converted to a 884-dimension vector. All the points are clustered with a K-means ++ clustering algorithm in 15 clusters. The corresponding clusters of the measurements of 3Aa are presented in b). The clusters showing plateaus are in colour boxes, and the ones showing no plateaus are in gray boxes. From the clusters showing a plateau, we extract a plateau length and conductance that are plotted in the graph c). Every data point corresponds to one cluster.

VII. Peptide conformations

In Fig. S7a, we show several possible conformations of a peptide. We consider the amide group as a partially planar structure that constitutes the repeating subunit of the peptide. Adjacent amide groups are connected through the α-carbon. There are two different conformations for amide groups connecting with adjacent α-carbons, *cis*- and *trans*- (Fig. S7b). For simplicity, in Fig. S7a we only show the *trans*-case. As the α-carbon has sp^3 hybridization, the amide groups can rotate around the α-carbon with an angle of about 110^o between two adjacent amide groups. This means that the peptide chain can fold and the degree of folding increases with peptide length. When the peptide length increases to 4Ala, it is possible that the C- and N- terminus get in close proximity to one another (see bottom right of Fig. S7a). Several different combinations may result in a similar overall conformation. Figure. S7a shows the case of MPA-(*n*)Ala, but if we replace some Ala units for Trp or Cys, the additional side chain would most likely result in additional, different conformations. Furthermore, the presence of both *cis*- and *trans*-amide groups, and the interaction of different peptide groups with the electrode gold surface will make the situation even more complex. All these factors explain the multiple short conductance plateaus observed in the experiments.

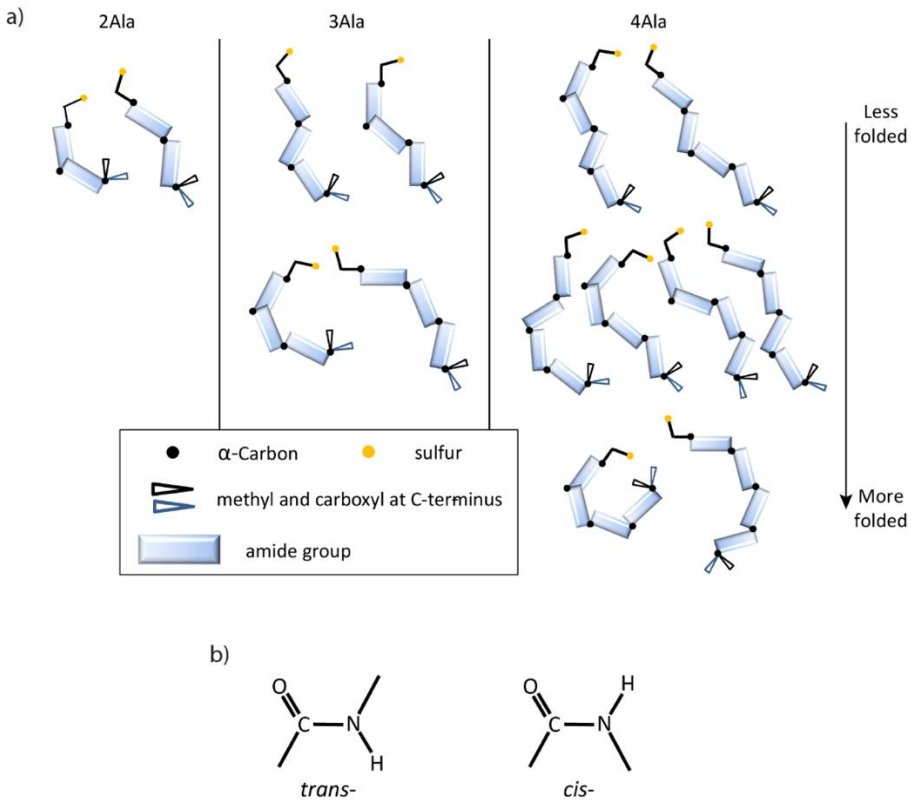

Figure S8. a) Some possible conformations of MPA-(*n*)Ala on Au electrode. All the amide groups are assumed to be *trans*- for simplicity. The conformations are sorted by their possible degree of folding. b) Trans- and cis-conformation of the amide group.

REFERENCES

1. Zotti, L A; Bednarz, B; Hurtado-Gallego, J; Cabosart, D; Rubio-Bollinger, G; Agrait, N; van der Zant, H S J, Can one Define the conductance of amino acids? *Biomolecules* **2019,** *9*, 580.
2. All data are available upon request to the authors.
3. Brisendine, J M; Refaely-Abramson, S; Liu, Z.-F; Cui, J; Ng, F.; Neaton, J B; Koder, R L; Venkataraman, L, Probing Charge Transport through Peptide Bonds. *J. Phys. Chem. Lett.* **2018,** *9*, 763-767.
4. Xiao, X Y; Xu, B ; Tao, N. J, Conductance titration of single-peptide molecules. *J. Am. Chem. Soc.* **2004,** *126*, 5370-5371.
5. Chen, F; Li, X L; Hihath, J; Huang, Z F; Tao, N J, Effect of anchoring groups on single-molecule conductance: Comparative study of thiol-, amine-, and carboxylic-acid-terminated molecules. *J. Am. Chem. Soc.* **2006,** *128*, 15874-15881.
6. Park, Y S; Whalley, A. C.; Kamenetska, M.; Steigerwald, M. L.; Hybertsen, M. S.; Nuckolls, C.; Venkataraman, L., Contact chemistry and single-molecule conductance: A comparison of phosphines, methyl sulfides, and amines. *J. Am. Chem. Soc.* **2007,** *129*, 15768-15769.
7. Salomon, A; Cahen, D; Lindsay, S; Tomfohr, J; Engelkes, V B; Frisbie, C. D, Comparison of electronic transport measurements on organic molecules. *Adv. Mater.* **2003,** *15*, 1881-1890.
8. Xu, B Q; Tao, N J, Measurement of single-molecule resistance by repeated formation of molecular junctions. *Science* **2003,** *301*, 1221-1223.